Long-lived nonlinear oscillatory states in interacting relativistic Bose-Einstein condensates

Leone Di Mauro Villari, Ian Galbraith, and Fabio Biancalana
Institute of Photonics and Quantum Sciences, School of Engineering and Physical Sciences, SUPA, Heriot-Watt University, Edinburgh EH14 4AS, United Kingdom

(Received 9 April 2020; accepted 20 August 2020; published 14 September 2020)

We study a mean-field model for the dynamics of an interacting Bose-Einstein condensate in two-dimensional pseudorelativistic materials. This model is relatively simple but contains long-lived solutions called oscillons which are absent in simple nonrelativistic condensates. We report on a variety of scenarios including interactions between pairs of oscillons and oscillons propagating across an inhomogeneous material boundary. Hitherto, relativistic oscillons have been studied only in high-energy physics and cosmology, and their relevance has not been highlighted so far in condensed-matter physics.

DOI: 10.1103/PhysRevA.102.033321

I. INTRODUCTION

Many decades after the theoretical prediction of Bose and Einstein, Bose-Einstein condensates (BECs) were experimentally detected in laser-cooled magnetically trapped ultracold bosonic atomic clouds [1–3]. More recently, BECs have also been seen in fermionic atomic gases as a result of fermions pairing into bosons [4]. An interesting and widely studied example of fermions pairing are the excitonic bound states of electron and holes in semiconductors. The possibility for semiconductor excitons to undergo Bose-Einstein condensation has been suggested long ago at the beginning of the 1960s [5]. As the critical temperature for elementary boson condensation scales as the inverse of the boson mass, it was thought that exciton condensation could be obtained at 100 K or even at room temperature, the exciton mass being much less than the free-electron mass. The experimental search for the condensed phase, however, turned out to be challenging mostly due to the fact that excitons are not an elementary but a composite boson with a finite lifetime [6]. Despite these difficulties, signatures of exciton condensation have been reported in double quantum wells [7–10], microcavities [11], graphene [12], and transition-metal dichalcogenoides [13]. It is known that excitons and exciton-polaritons show a BEC-like insulating phase, that has been the subject of promising theoretical and experimental investigation mainly in graphenelike real [14–16] and synthetic [17] lattices as well as in topological insulators [18]. This BEC-like phase is particularly interesting from experimental and theoretical points of view since it presents the crossover behavior from the Bardeen-Cooper-Schrieffer (BCS) limit to the Bose-Einstein condensation limit. Recently, exciton condensates with superfluids transport properties have been observed in double bilayer graphene [19] and van der Waals heterobilayers [20]. Due to the pseudorelativistic behavior of low-energy quasiparticles in a honeycomb lattice, one may wonder what are the relevant properties of the dynamics in the condensed phase. Moreover the relevance of relativistic BECs has been recently pointed out in gases with both electron and hole pairings. Relativity comes into play as those two composite bosons form a particle antiparticle pair [3]. The boson-boson interaction in relativistic BECs could be potentially used to experimentally mimic field theory in condensed matter. It is also a promising system for the analog model of gravity [21].

In this paper, starting from the dispersion of excitons in Dirac-like materials, we derive and investigate a simple but flexible mean-field model that can describe the dynamics of the condensed phase in different physical scenarios. Central to this model is a relativistic generalization of the Gross-Pitaevskii equation (GPE), i.e., a nonlinear Klein-Gordon equation (NLKGE). In Sec. II, we derive the exciton dispersion relation using a two-particle model. In Sec. III, we study the condensate phase of the exciton and derive the mean-field model. In Sec. IV, we investigate the properties of a nonstationary but localized solution of the model, known as an oscillon. In Secs. V and VI, we study the oscillon dynamics in more complicated scenarios: When they interact with each other and with a localized defect and when two materials with different energy gap are in contact. Until now, the oscillon solutions of relativistic field theories have been studied only in high-energy physics and cosmology, in particular, for self-interacting scalar fields and in the SU(2) Higgs model [22]. Oscillon solutions exist also in nonrelativistic BECs, but their mathematical structure is different. In such systems, in order to stabilize oscillating solutions, one needs to either consider coupled equations or apply some sort of external perturbation. A discussion of nonrelativistic oscillon solutions in BECs can be found in Refs. [23,24]. In these papers, the authors consider coupled BECs [23] and a system confined in a trap with oscillating walls [24]. Oscillons in nonlinear and parametrically driven systems have been studied and experimentally observed in fluids, such as granular media [25], Newtonian fluids [26], and colloidal suspensions [27]. The formation and interaction of oscillons have been the subject of several theoretical, numerical, and experimental studies. However, a number of open problems remains mostly related to their

stability and to the transition between radiative and nonradiative oscillons. Recent papers studying parametrically driven systems in one dimension focused on the transition between localized structures to breathing localized states [28,29]. In two dimensions, oscillon instabilities have been numerically studied in magnetic systems [30] and in the parametrically driven damped sine-Gordon equation [31].

II. EXCITON DISPERSION IN DIRAC MATERIALS

The Hamiltonian describing the low-energy behavior of Dirac quasiparticles around one K point of the reciprocal honeycomb lattice reads

$$H_1 = \begin{pmatrix} \Delta/2 & vpe^{i\theta} \\ vpe^{-i\theta} & -\Delta/2 \end{pmatrix}, \tag{1}$$

where Δ is the energy gap and v is the Fermi velocity, $p = \hbar k$ is the modulus of the electron momentum, and $\theta = \arctan(p_y/p_x)$. Such dispersion is appropriate to describe low-energy electrons in gapped graphene and, with certain limitations, transition-metal dichalcogenides (TMDs). Assuming zero center-of-mass momentum for excited e-h pairs, the two-particle Hamiltonian without Coulomb interaction is given by the tensor product $H_2 = H_1 \otimes I_2 - I_2 \otimes (TH_1T^{-1})$ with I_2 as the 2×2 identity matrix and T as the time-reversal operator. It reads

$$H_2 = \begin{pmatrix} 0 & vpe^{i\theta} & vpe^{-i\theta} & 0 \\ vpe^{-i\theta} & \Delta & 0 & vpe^{-i\theta} \\ vpe^{i\theta} & 0 & -\Delta & vpe^{i\theta} \\ 0 & vpe^{i\theta} & vpe^{-i\theta} & 0 \end{pmatrix}, \tag{2}$$

and this matrix has four eigenvalues: $\pm 2\sqrt{v^2p^2 + \Delta^2/4}$ and a doubly degenerate zero eigenvalue [15]. The zero-energy eigenstates correspond to the cases when the system has a single electron or a hole with its complementary particle in the negative energy sea [15,32].

III. CONDENSATE STATES OF EXCITONS

To study condensed phases in a Dirac material, the Hamiltonian in Eq. (2) needs to be modified to include Coulomb interactions [15]. They can be introduced by deriving a set of renormalized Dirac-Bloch equations [16,33–36]. When electrons and holes have the same mass, the Hamiltonian in Eq. (2) can be block diagonalized [32]. We set up the bands in such a way that zero energy is located halfway between their extrema. This results in a reduced electron-hole Hamiltonian [15],

$$H_E = \begin{pmatrix} \Delta/2 & vqe^{i\theta_q} \\ vqe^{-i\theta_q} & -\Delta/2 \end{pmatrix}, \tag{3}$$

where $q = |\mathbf{q}|$ is the modulus of the exciton's momentum in the center-of-mass frame and θ_q is the related angle [15]. After introducing Coulomb interaction, the eigenvalue problem for the Hamiltonian H_E can be solved analytically giving the exciton energies and wave functions [36,37]. The energy levels of the exciton series are given by

$$E_{n,j} = \frac{\Delta}{\sqrt{1 + \frac{\alpha_c^2}{(n+\gamma)^2}}}, \tag{4}$$

where n is the principal quantum number and $\gamma = \sqrt{j^2 - \alpha_c^2}$ with $j = m + 1/2$ being the eigenvalue of the pseudo-spin-angular momentum. The constant α_c is the dimensionless Coulomb coupling strength and the spinor wave function is of the form

$$\vec{\Psi}_{n,j}(\mathbf{q}) = \begin{pmatrix} \varphi_{n,j}(\mathbf{q}) \\ \pm i\chi_{n,j}(\mathbf{q}) \end{pmatrix}. \tag{5}$$

From Eq. (4), we can observe that if the coupling constant exceeds the critical value ($\alpha_c = \frac{1}{2}$), the ground-state energy becomes imaginary and a phase transition to an excitonic insulator occurs [16]. The excitonic insulator state is a BCS-like condensate of excitons that can show a BCS-BEC crossover at low density [38]. It can be regarded as a coherent superposition of the noninteracting ground state and all exciton states with vanishing real parts of the lowest-energy level $E_{0,1/2}$ [16]. This state is more complicated than a normal BEC since, at strong Coulomb coupling, the quasiparticle picture becomes less accurate and the many-body theory may be needed. A description of this state at the mean-field level at low density is presented in Ref. [39]. In what follows, we focus on the low Coulomb interaction regime $\alpha_c < 1/2$ where the use of the excitonic limit is more appropriate. In this regime, the ground state for the excitons is the normal $1s$ state, and the system can undergo a phase transition to a BEC state when cooled below a critical temperature T_c. For exciton systems, this temperature can be around 100 K or higher [6]. A detailed description of the macroscopic coherent ground state of an exciton condensate is given in Chap. 2 of Ref. [40]. We will now derive the mean-field model that describes the dynamics of the condensate state. We consider X^0-type excitons only with spin and pseudospin both equal to zero.

In the low-density limit, the system can be seen as a weakly interacting Bose gas of excitons. The noninteracting first quantized Hamiltonian of a pseudorelativistic gas of bosons reads

$$H_0 = \sqrt{\hbar^2 v^2 \hat{k}^2 + m^2 v^4}, \tag{6}$$

where $\hat{k}$ is the momentum operator and $m = \hbar^2(d^2\mathcal{E}_k)/dk^2)^{-1} = \Delta/(4v^2)$ is the exciton effective mass with $\mathcal{E}_k$ being the exciton dispersion. In relativistic quantum mechanics, Dirac proved the equivalence between the ill-defined operator H_0 and Hamiltonian H_E for spin-1/2 massive particles. The same equivalence can be established also for scalar particles by regarding the scalar wave field as a doublet. A detailed explanation of this can be found in Sec. 4 of Ref. [41].

To simplify our treatment, we approximate the exciton-exciton interaction with a hard-sphere potential [40,42],

$$\mathcal{U}(\mathbf{r} - \mathbf{r}') = N\frac{4\pi\hbar^2}{mL_{\text{eff}}}a_B\delta(\mathbf{r} - \mathbf{r}'), \tag{7}$$

where a_B is the $1s$ exciton Bohr radius, L_{eff} the effective thickness of the monolayer and N the number of particles. The use of this approximation for the interaction potential is justified within the low-density limit ($n_{\text{ex}}a_B^2 \ll 1$). In other words, since the excitons are neutral when the density is low enough to ignore the fermionic nature of the electron-hole pairs, one can assume that the range of interactions is on the order of the exciton Bohr radius.

Within this approximationn we can compute the field Hamiltonian from H_0 and the interacting potential in Eq. (7). We define first the exciton creation operator in one of the two equivalent K points using the spinor in Eq. (5),

$$\hat{c}^\dagger_{\mathbf{k}} = \sum_{\mathbf{q}} [\varphi(\mathbf{q}) + i\chi(\mathbf{q})]\hat{a}^\dagger_{\mathbf{k}+\mathbf{q}}\hat{b}^\dagger_{\mathbf{k}-\mathbf{q}}, \tag{8}$$

where $\{\hat{a}^\dagger_k, \hat{b}^\dagger_k, \hat{a}_k, \hat{b}_k\}$'s are the ladder operator for electrons and holes. More details on the definition of the exciton operator are given in Appendix A. We drop the (n, j) indices since we are considering condensed excitons in the ground state. The field operator for this type of pseudorelativistic scalar excitons is written as

$$\hat{\phi}(\mathbf{r}, t) = \frac{1}{\sqrt{A}} \sum_{\mathbf{k}} \frac{1}{\sqrt{\mathcal{E}_{\mathbf{k}}}} (\hat{c}_{\mathbf{k}} e^{-i(\mathbf{k}\cdot\mathbf{r}-\omega_{\mathbf{k}}t)} + \hat{c}^\dagger_{\mathbf{k}} e^{i(\mathbf{k}\cdot\mathbf{r}-\omega_{\mathbf{k}}t)}), \tag{9}$$

where A is the area of the layer. We can now use this field operator and Eqs. (6) and (7) to compute the field Hamiltonian as

$$H(\hat{\phi}) = \int d^2r\, \hat{\phi}(\mathbf{r}) \left(i\hbar \frac{\partial}{\partial t} - H_0 \right)^2 \hat{\phi}(\mathbf{r}) + \int d^2r\, d^2r' \hat{\phi}(\mathbf{r})\hat{\phi}(\mathbf{r}')\mathcal{U}(|\mathbf{r}-\mathbf{r}'|)\hat{\phi}(\mathbf{r})\hat{\phi}(\mathbf{r}'), \tag{10}$$

where we have squared the linear term, a standard procedure in high-energy physics to derive the Klein-Gordon Hamiltonian from the pseudodifferential operator H_0. After some algebra, we obtain a pseudorelativistic generalization of the GPE [21],

$$H(\hat{\phi}) = \frac{1}{2} \int d^2r [\hbar^2 \hat{\phi}_t^2 + \hbar^2 v^2 (\nabla\hat{\phi})^2 + m^2 v^4 \hat{\phi}^2 + 2U_0 \hat{\phi}^4]. \tag{11}$$

Here, $U_0 = N4\pi\hbar^2 m v^4 a_B / L_{\text{eff}}$, and this nonlinear coupling constant has dimensions of energy cubed × area. The Hamiltonian in Eq. (11) is Lorentz invariant with velocity v, the Fermi velocity of the carriers. The mismatch between the Fermi velocity and the speed of light will break the Lorentz invariance when the system is coupled with an external electromagnetic field. We should expect the same symmetry breaking at high density beyond the validity of the excitonic limit. In this case, the Fermi nature of electrons and holes is relevant, and the dipole interaction would again break Lorentz invariance. Hamiltonians in Eqs. (1) and (3) are first order in the low-momentum ($\mathbf{kk}\cdot\mathbf{p}$) expansion around the K point. It is worth stressing, here, that higher-order terms, such as trigonal warping and electron-hole asymmetry, can break Lorentz invariance [43]. It has been shown, however, that these distortions of the band structure are negligible in graphene and many graphenelike systems, thus, the Dirac quasiparticle picture is appropriate in many realistic situations. This makes the derivation of Eq. (11) consistent with real world experiments [43].

In terms of ladder operators, the Hamiltonian in Eq. (11) can be written as (see Appendix B),

$$H = \sum_{\mathbf{k}} \mathcal{E}_{\mathbf{k}} \hat{c}^\dagger_{\mathbf{k}} \hat{c}_{\mathbf{k}} + \frac{U_0}{2A} \sum_{\mathbf{klp}} \frac{1}{\sqrt{\mathcal{E}_{\mathbf{k}}\mathcal{E}_{\mathbf{l}}\mathcal{E}_{\mathbf{l}+\mathbf{p}}\mathcal{E}_{\mathbf{k}-\mathbf{p}}}} \hat{c}^\dagger_{\mathbf{k}} \hat{c}^\dagger_{\mathbf{l}} \hat{c}_{\mathbf{l}+\mathbf{p}} \hat{c}_{\mathbf{k}-\mathbf{p}}, \tag{12}$$

where the second term is the standard four-field interaction commonly used to model the condensed phase of an interacting gas of excitons in the structureless particle approximation [40], namely, when we can neglect the fermionic nature of the electron-hole pairs. The energy-dependent prefactor comes from the normalization of the exciton scalar field. When the bosons are in a condensate state, it is then possible to describe the dynamics of the condensate at the mean-field level by performing the substitution $\hat{\phi}(t) \to \phi(t)$: The order parameter ϕ satisfies then the classical equation,

$$\Box\phi - \mu^2\phi - \tilde{U}_0\phi^3 = 0, \tag{13}$$

with $\mu = mv/\hbar$, $\tilde{U}_0 = U_0/\hbar^2 v^2$, and we adopted the standard definition for the flat space box operator,

$$\Box = -\frac{1}{v^2}\partial_t^2 + \nabla^2, \tag{14}$$

with the Fermi velocity v. Equation (13), in $2+1$ dimensions has nonstationary localized solutions called oscillons [22, 44–46]. Oscillons are metastable solutions with a very long lifetime that depends critically on the initial condition [44–46]. The longevity of the oscillon lifetime has been extensively reported in many numerical studies [22,44,46] along with their solitonlike properties [44,45]. In the following sections, we will review some of these properties and explore further aspects of these solutions. Before proceeding to the solution of Eq. (13), we will give a brief summary on its validity. Being a generalization of the GPE, Eq. (13) retains its limitations, the exciton-exciton four-fields interaction is valid either in the diluted regime in consideration here or in the opposite limit (high density) when the coupling is very weak $U_0 \approx 1/N$, where $N \gg 1$ is the number of excitons. Moreover, this formulation holds when finite temperature effects are negligible. We note that a finite temperature may be included in the mean-field picture with a simple modification of Eq. (11) [47].

IV. OSCILLONS IN RELATIVISTIC BECS

In this section, we first review the emergence of oscillons in the nonlinear Klein Gordon equation in Eq. (13) [44–46]. We, then, discuss the relation between the dispersion term and the oscillon's formation. To do so, we introduce a system of scaled space and time variables given by

$$\xi = \frac{x}{x_0}, \quad \eta = \frac{y}{y_0}, \quad \tau = \frac{t\Delta}{\hbar}, \tag{15}$$

and define $r_0 = \sqrt{x_0^2 + y_0^2}$. x_0 and y_0 are chosen appropriately for the initial conditions of the problem, and, for our purposes, we always choose $x_0 = y_0$. In these variables, Eq. (13) reads

$$\partial_\tau^2\psi - \beta\left(\partial_\xi^2 + \partial_\eta^2\right)\psi + \psi + \psi^3 = 0, \tag{16}$$

where $\beta = 8[\hbar v/(r_0\,\Delta)]^2$ and the dimensionless field $\psi(\xi, \eta, \tau)$ is defined as

$$\psi = 4\hbar v \sqrt{\frac{N\pi a_B}{L_{\text{eff}}\Delta}}\phi. \tag{17}$$

Equation (16) has been solved using both a pseudospectral implicit method and a finite difference leapfrog algorithm

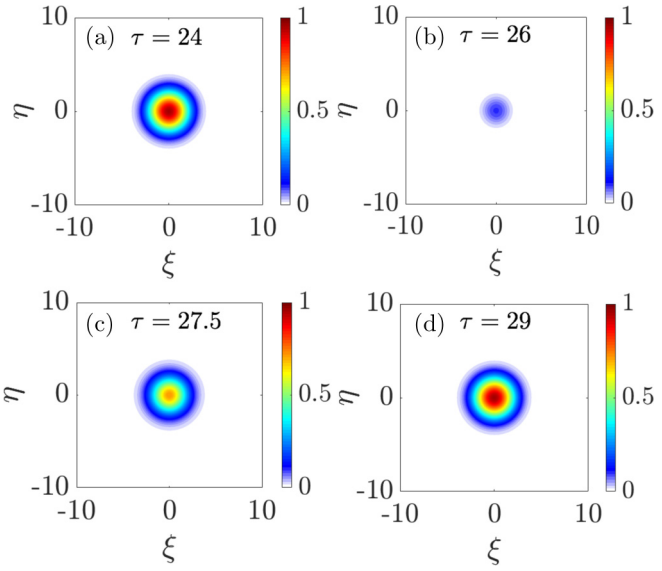

FIG. 1. Dynamics of the modulus square of the field, in time, after subtracting the background. (a) The initial oscillon state, (b) the first collapse, and (c) and (d) the first revival. The first snapshot is at $\tau = 24$ after the initial transient has quenched.

[44]. In what follows, we present the results for a gapped graphene sample $\Delta = 0.2$ eV, $v = c/300$, and $\beta = 1$, which implies $r_0 = 9.3$ nm. Figure 1 shows the dynamics of the modulus square of the field ψ when the initial state comprises a uniform condensate background with a Gaussian-shaped hole at the origin, i.e.,

$$\psi(\xi, \eta) = A_0(1 - e^{-(\xi^2+\eta^2)/\sigma^2}), \tag{18}$$

with $A_0 = 1$ and $\sigma = 2.86$ which is chosen so that the oscillon solution is maximally metastable [44,45], i.e., it has the maximal lifetime. This means that, in this configuration, the nonlinearity best compensates the dispersion. We note that a satisfactory explanation for the metastability of oscillon solutions is still missing. There is not an obvious relation between the long lifetime of the oscillon and the symmetries of the Hamiltonian. This is due to the fact that the NLKGE is not integrable, and, thus, there is no direct link between its solutions and conservation laws. However, we know that, in nonrelativistic systems, localized solutions with periodic oscillations are not attractors of the dynamic unless one considers more complicated systems [23,24] as we have mentioned in the Introduction. This suggests that the pseudorelativistic nature of the Hamiltonian plays an important role in the formation of the long-living oscillon. There have been attempts in the literature to relate the long lifetime with adiabatic invariance, but this approach just takes into account very weak nonlinearities [48]. It was also proposed but without a rigorous proof that a Lyapunov exponent governs the power law of the oscillon lifetime [46].

In Fig. 1, we show the dynamics of the square modulus of the oscillon field, after subtracting the background (A_0), we can see after one period the original peak is fully recovered. These oscillating dynamics are quite resilient as we can see in Fig. 2(a), even if it suffers from a weak breathing effect due to the nonintegrability of the system. This is in agreement

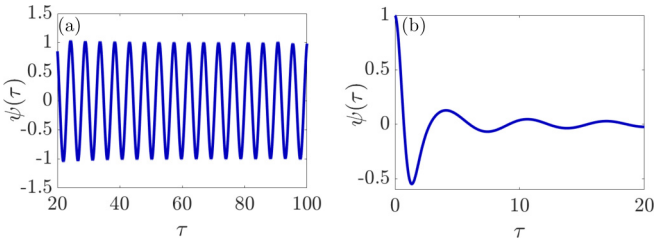

FIG. 2. (a) The oscillon field in the time domain at $(\xi, \eta) = (0, 0)$ for $A_0 = 1$ and $\sigma = 2.86$. (b) The dispersive solution at $(\xi, \eta) = (0, 0)$ for $A_0 = 1$ and $\sigma = 1$.

with previous results in the literature [44–46]. In contrast, in Fig. 2(b), we can see the propagation of a dispersive solution ($A_0 = 1$ and $\sigma = 1$). Our numerical simulations as well as previous results [44–46] show that the lifetime of the solution depends critically on the initial condition, and it is determined by the standard deviation σ of the Gaussian ansatz. A deeper understanding of why, for specific values of σ, the dynamics evolves into an oscillon would come from a rigorous exploration of the metastability of these solutions.

It is interesting to study the effect of the dispersion on the dynamics of the oscillon by varying the width of the initial Gaussian hole. In Fig. 3, we can see how the dispersion mostly affects the early stage of the dynamics. When we increase r_0, the dispersion term becomes less important, and the formation of the oscillon is considerably delayed as we can clearly see from Figs. 3(b) and 3(c). In Fig. 3(d), the dynamics completely changes, as the dispersion becomes completely negligible, and the field at (0,0) oscillates only slightly around the minimum ($\psi = 0$)—note the axis scale change. The oscillations of the background, instead, are driven by the amplitude of the field only as expected in the strong nonlinear limit (see Fig. 4).

In Fig. 4, we can see that the oscillon's frequency increases with the strength of the initial field, that also defines the

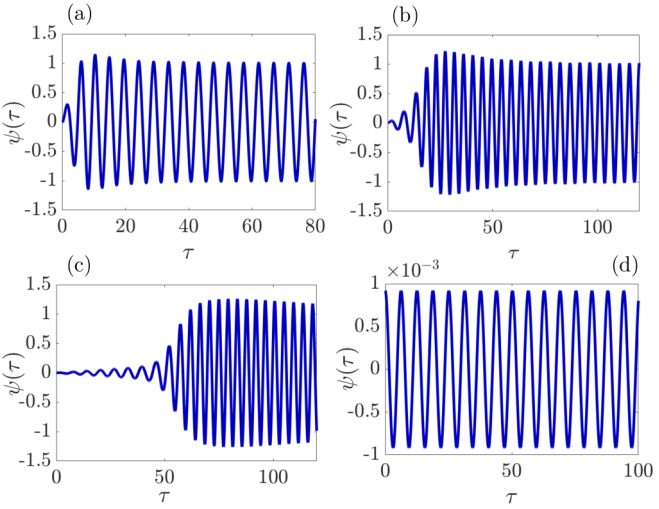

FIG. 3. Early stage dynamics of the oscillon field at $(\xi, \eta) = (0, 0)$ for decreasingly dispersive (increasing r_0, hence, decreasing β) cases. (a) $r_0 = 9.3$ nm (hence, $\beta = 1$), (b) $r_0 = 29.4$ nm ($\beta = 10^{-1}$), (c) $r_0 = 93.2$ nm ($\beta = 10^{-2}$), (d) $r_0 = 29.4$ μm ($\beta = 10^{-7}$).

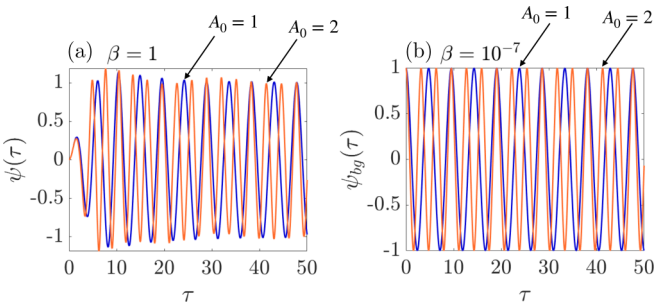

FIG. 4. (a) Dynamics of the oscillon for two condensate densities, $A_0 = 1$ (blue) and $A_0 = 2$ (orange). (b) Oscillations of the background for the dispersionless equation again for $A_0 = 1$ (blue) and $A_0 = 2$ (orange).

strength of the nonlinearity. This is a well-known nonlinear effect called self-phase modulation.

To inform experimental considerations of this system, it is important to estimate some relevant physical quantities. The period of the oscillon is particularly significant because excitons are not simple bosons, but composite quasiparticles with a finite lifetime and a period longer than that would be impossible to observe. This quantity can be computed from Fig. 1 and the scaling relation Eq. (15), we get $T = 20$ fs that is well below the exciton lifetime in two-dimensional materials that is on the order of a few picoseconds up to 150 ps [49]. Our model relies on the assumption of the low-density limit regime, thus, an important quantity is the exciton density. From the interaction strength U_0, we can calculate the density for an oscillon with initial amplitude $A_0 = 1$ and radius $r_0 = 9.3$ nm as $n_{\rm ex} = 3.16 \times 10^{11}$ cm^{-2} which, combined with the exciton Bohr radius, gives $n_{\rm ex} a_B^2 = 0.16$ confirming the low-density requirement is met. In particular, for a system with a 0.2-eV gap and Coulomb coupling constant $\alpha_c = 0.47$, we have a $1s$ state binding energy $\epsilon_b = 0.07$ eV and Bohr radius $a_B = 6.68$ nm.

V. OSCILLON INTERACTIONS

In nonlinear partial-differential equations, such as Eq. (16), specific behaviors arise from the subtle interplay between nonlinearity and dispersion. In most cases, this is a matter of the specific numbers involved, and in this section and the next, we illustrate two scenarios, namely, oscillon collisions and the effect of heterostructures on oscillons. The underlying physics in both cases is essentially the same as is explained as in the first sections on oscillon physics.

We review first the collision of two identical oscillons [44] moving along the diagonal, then, we study the interaction between the oscillon and a defect. In the case of collision, the initial state reads

$$\psi(\xi,\eta) = A_0\Bigg(2 - \exp\left[-\frac{(\xi-\xi_0)^2 + (\eta-\eta_0)^2}{\sigma^2}\right] - \exp\left[-\frac{(\xi-\xi_1)^2 + (\eta-\eta_1)^2}{\sigma^2}\right]\Bigg). \quad (19)$$

As shown in Fig. 5, the solitonlike behavior of the solution is preserved after the collision. It is also interesting to see

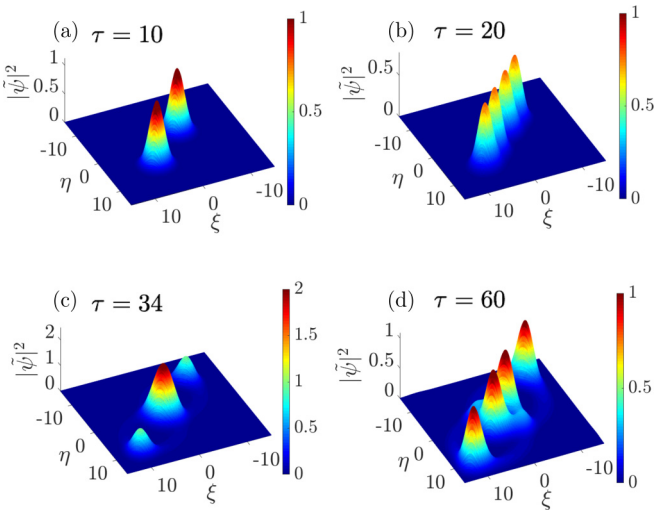

FIG. 5. Scattering of two oscillons of initial amplitude $A_0 = 1$, $\sigma = 2.86$ and initial speed $\tilde{v}_0 = 0.5$. (a) Initial state of the oscillon, (b) separation of positive and negative energies, (c) collision time, and (d) final state after collision. Here, with $\tilde{\psi}$, we indicate the field after subtracting the background.

how the oscillons interact with a defect of the condensate. This can be simulated by adding a loss term, proportional to the first time derivative of the field. Equation (16) is modified as follows:

$$\partial_\tau^2\psi - \beta(\partial_\xi^2 + \partial_\eta^2)\psi + \psi + \psi^3 + \Gamma(\xi,\eta)\partial_\tau\psi = 0, \quad (20)$$

and we consider a Gaussian defect of the form [50]

$$\Gamma(\xi,\eta) = \Gamma_0 \exp\left(-\frac{(\xi-\xi_d)^2 - (\eta-\eta_d)^2}{\sigma_d^2}\right), \quad (21)$$

where Γ_0 is the strength of the damping and $\{\xi_d, \eta_d\}$ is the coordinates of the defect. In Fig. 6, we observe that the oscillon is resilient even to nonperturbative damping ($\Gamma_0 \gg 1$).

The scaled initial speed $\tilde{v}_0$ we used in in this section corresponds to a velocity $v_0 = 0.5\,v$. Solitons with a velocity close to the local speed of sound are known to be experimentally more stable and easier to produce in atomic nonrelativistic systems. This would be a very interesting aspect to study experimentally in pseudorelativistic materials where the role of the local speed of sound is played by the Fermi velocity v. Recently, it has been proposed as an experiment with controllable near-zero soliton velocity in atomic BEC [51]. It would be very interesting, ideally, with a setup that is able to control the oscillon velocity to study both the low velocity and, in principle, the ultrarelativistic limit $v_0 = v$.

VI. CONDENSATES IN HETEROLAYERS

We now investigate BECs spanning two connected Dirac material slabs with different energy gaps (Δ_1 and Δ_2) requiring an adapted version of Eq. (16). To do so, we introduce a scaled time as $\tau = t\Delta_1/\hbar$. This leads to a dimensionless equation that has the same form as Eq. (16) on the side with energy gap Δ_1 and mass $m_1 = \Delta_1/4v^2$ and that depends on the ratio between two different energy gaps $\Delta_2/\Delta_1 = m_2/m_1$

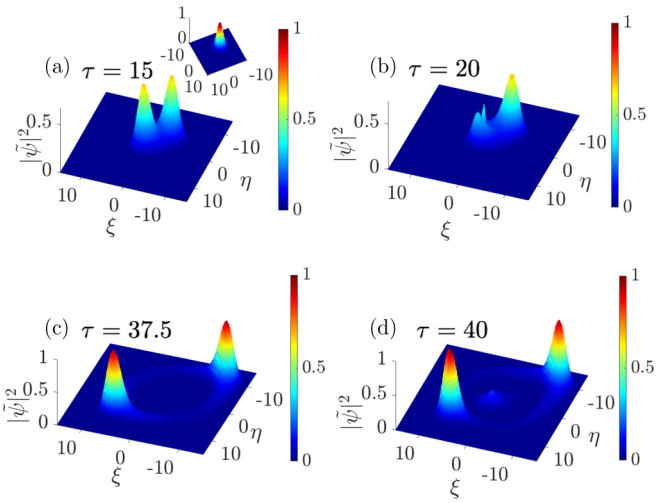

FIG. 6. Interaction of a single oscillon with a Gaussian-shaped defect located at $(\xi, \eta) = (0, 0)$ and $\Gamma_0 = 50$, $\sigma_d = 10^{-2}$. (a) Early stage of the dynamics: separation of positive and negative energies. (b) Interaction with the defect and (c) and (d) late stage of the dynamics. The inset in (a) is the initial state of the oscillon $A_0 = 1$ and $\tilde{v}_0 = 0.5$.

on the other side,

$$\partial_\tau^2 \psi - \beta\left(\partial_\xi^2 + \partial_\eta^2\right)\psi + \gamma^2(\xi)\psi + \gamma(\xi)\psi^3 = 0,$$
$$\psi(\xi, \eta, 0) = \psi_0(\xi, \eta), \quad (22)$$

where $\beta = 8[\hbar v/(r_0\,\Delta_1)]^2$ and the scaled field ψ is defined as in Eq. (17) with $\Delta = \Delta_1$. The space-dependent coefficient $\gamma(\xi)$ is defined as follows:

$$\gamma(\xi) = 1, \quad \xi < 0,$$
$$\gamma(\xi) = \frac{\Delta_2}{\Delta_1}, \quad \xi > 0. \quad (23)$$

We take first the simplest case of a constant background $\psi_0(\xi, \eta) = \psi_0$. As we can see from Fig. 7, traveling waves are generated by scattering at the boundary between the two

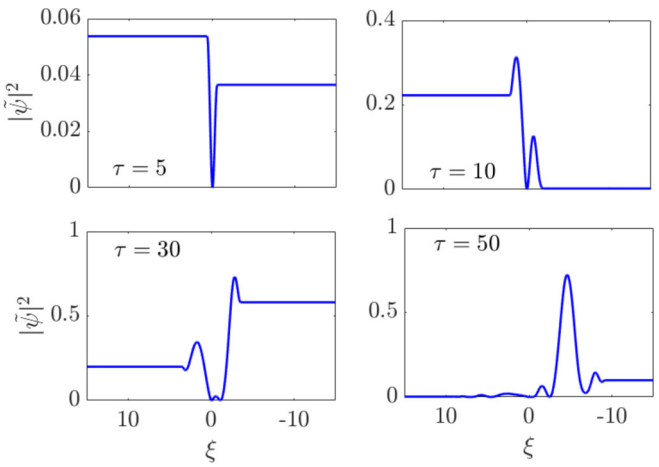

FIG. 7. Motion of traveling waves in two condensates with $\Delta_1 = 0.2$ and $\Delta_2 = 0.3$ eV and constant background $\psi_0(\xi, \eta) = 1$.

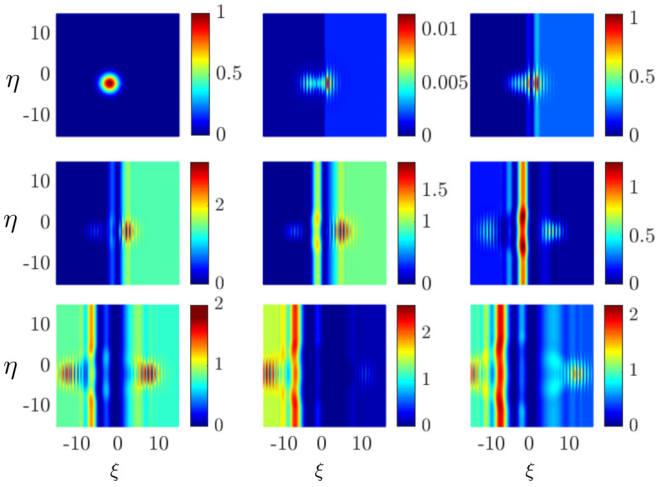

FIG. 8. Motion of an oscillon between two condensates with $\Delta_1 = 0.2$ and $\Delta_2 = 0.3$ eV. The initial state $\psi_0(\xi, \eta)$ is a Gaussian well of the form Eq. (18) located at $(\xi, \eta) = (-2, -2)$ with $A_0 = 1$ and $\sigma = 2.86$. The sequence of snapshots from left to right in each row is as follows: $\tau = 0.2, 2.3, 4.4, 6.7, 9, 11.2, 13.5, 15.7, 18$.

layers and propagate throughout the two sides of the condensate. The dynamics of these waves is straightforwardly understood using a multiple scale perturbative analysis of Eq. (22) limited to one side of the heterolayer (see Appendix C for details). In Fig. 8, we show the motion of an oscillon located initially in the condensate with energy gap Δ_1. The stability of the oscillon dynamics is not particularly influenced by the presence of the second condensate after the splitting of positive and negative energies. The oscillon moves through the second condensate and starts oscillating with a higher frequency proportional to the second gap Δ_2 as we show in Fig. 9. From Fig. 9, we can compute the frequency (in eV) of the first harmonics of the oscillons on both sides of the condensate. We get $\omega_1 = 0.041$ and $\omega_2 = 0.068$ eV. Those values are significantly lower than the two energy gaps (Δ_1

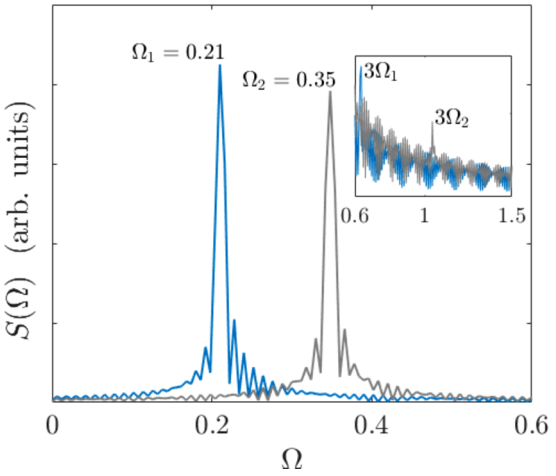

FIG. 9. Oscillon spectrum on both sides of the heterolayer $\xi < 0$ (blue, lower-frequency peak) and $\xi > 0$ (gray, higher-frequency peak). Ω is a dimensionless frequency related to the inverse of τ. The inset: third-harmonic generation.

and Δ_2) in the two sides of the heterolayer, this is because we are studying the dynamics of the system at a relatively early stage between $\tau = 10$ and $\tau = 200$ when the combined effect of the dispersion and the nonlinearity is still strong. For long-time propagation, the value of the frequency approaches the one of the energy gap and the system behaves, such as a harmonic oscillator [44]. In the inset, we can observe the generation of third harmonics in the spectrum of the bosonic field as expected from a system with third-order nonlinearity. This effect is clearly not specifically related to the heterolayer structure studied in this section and would be present in the spectrum of the time series in Figs. 2–4.

VII. CONCLUSIONS

In this paper, we derived a simple mean-field model to investigate the dynamics of Bose-Einstein condensates for a quasiparticle with pseudorelativistic low-energy dispersion. This approach is based on a generalization of the Gross-Pitaevskii equation. We applied this model to the exciton dispersion of gapped Dirac material, such as doped or strained graphene and TMDs. We remark, however, that the interest of this model is not limited to these materials but could be applied to other physical systems. Magnons in $TlCuCl_3$ [52], for example, have been proven to show a BEC phase with a relativistic dispersion relation. It could be also be generalized by including the polarization degree of freedom to exciton-polariton condensates in synthetic honeycomblike photonic lattices. We studied the properties of a nonstationary but localized solution of the model, known as an oscillon. We detailed the dynamics of the two-oscillons interaction and proved that this solution is also resilient to the interaction with impurities of the background. Until now, the relevance of oscillon solutions of relativistic field theories has been highlighted only in high-energy physics in both $2+1$ and $3+1$ dimensions, and they have not been considered in condensed-matter physics. It is important to note that the oscillon solutions we have discussed in this paper are not allowed in simple nonrelativistic BECs because the Gross-Pitaevskii is first order in time. They are tightly related to the pseudorelativistic dispersion of Dirac quasiparticles. As we mentioned in the Introduction, oscillons of a different mathematical structure can be found in coupled nonrelativistic systems or in cavities with oscillating walls. Materials that show a BEC phase with the pseudorelativistic dispersion relation could represent an interesting optical analog platform to experimentally mimic field theories.

ACKNOWLEDGMENTS

L.D.M.V. acknowledges support from the EPSRC Centre for Doctoral Training in Condensed Matter Physics (Grant No. EP/G03673X/1) and wishes to thank Dr. D. N. Carvalho (NORDITA) for useful early discussions.

APPENDIX A: WANNIER EQUATION AND THE EXCITON OPERATOR

In this Appendix, we give more details on the Wannier equation for excitons in pseudorelativistic materials. Assuming the noninteracting ground state, the linear-response Dirac-Bloch equation for the polarization P_k is given by [16,33–36]

$$i\hbar\dot{P}_{\mathbf{k}} = 2\left(\epsilon_{\mathbf{k}} + \frac{1}{2}\sum_{\mathbf{k}'} V_{\mathbf{k}\mathbf{k}'}\right)P_{\mathbf{k}} - \hbar\Omega^R(t), \tag{A1}$$

where ϵ_k is the electron and hole pseudorelativistic dispersion and $\Omega^R(t)$ is the Coulomb-renormalized Rabi frequency. The related Wannier equation (electron-hole Coulomb problem) reads [15,16,53]

$$2\epsilon_{\mathbf{k}} u_{n,j}(\mathbf{k}) + \sum_{\mathbf{k}'} V_{\mathbf{k}\mathbf{k}'} u_{n,j}(\mathbf{k}) = E_{n,j} u_{n,j}(\mathbf{k}), \tag{A2}$$

this equation corresponds to the k-space representation of the Dirac-Coulomb problem [15,16,37,53],

$$(2\hbar v\boldsymbol{\sigma}\cdot\mathbf{k} + \Delta\sigma_z + V(\mathbf{r}))\vec{\Psi}_{nj}(\mathbf{r}) = E_{n,j}\vec{\Psi}_{nj}(\mathbf{r}), \tag{A3}$$

where $\vec{\Psi}_{nj}($ is a two-components spinor. Equations (A2) and (A3) have, in principle, both positive and negative energy solutions. When we consider X^0 paraexcitons, they are simply the complex conjugate of each other. The positive energy solutions of Eq. (A2) are given by [16]

$$u_j(\mathbf{k}) = \varphi_j(\mathbf{k}) + i\chi_j(\mathbf{k}), \tag{A4}$$

where $\varphi_j(k)$ and $i\chi_j(k)$ are the spinor components in k space where we dropped the index n and we fixed the pseudo-spin-angular momentum $j = \pm 1/2$. The exciton creation operator can be written as

$$\hat{c}^\dagger_{\mathbf{k}} = \sum_{\mathbf{q},j} u_j(\mathbf{q})\hat{a}^\dagger_{\mathbf{k}+\mathbf{q},j}\hat{b}^\dagger_{\mathbf{k}-\mathbf{q},-j}. \tag{A5}$$

APPENDIX B: THE PSEUDORELATIVISTIC HAMILTONIAN IN MOMENTUM SPACE

In this second Appendix, we show how to relate the pseudorelativistic Hamiltonian in Eq. (11) with the momentum space Hamiltonian in Eq. (12) of the main text. It is easier to deal with the interacting and noninteracting terms separately. We first rewrite the linear Hamiltonian H_0,

$$H_0 = \frac{1}{2}\int d^2r[\hbar^2\hat{\phi}_t^2 + \hbar^2 v^2(\nabla\hat{\phi})^2 + m^2v^4\hat{\phi}^2], \tag{B1}$$

using the expansion in terms of exciton ladder operators,

$$\hat{\phi} = \frac{1}{\sqrt{A}}\sum_{\mathbf{k}}\frac{1}{\sqrt{\mathcal{E}_{\mathbf{k}}}}(\hat{c}_{\mathbf{k}}e^{-i(\mathbf{k}\cdot\mathbf{r}-\omega_{\mathbf{k}}t)} + \hat{c}^\dagger_{\mathbf{k}}e^{i(\mathbf{k}\cdot\mathbf{r}-\omega_{\mathbf{k}}t)}), \tag{B2}$$

substituting this expression in Eq. (B1), after lengthy but simple algebra [54], we get

$$H_0 = \sum_{\mathbf{k}}\mathcal{E}_{\mathbf{k}}\hat{c}^\dagger_{\mathbf{k}}\hat{c}_{\mathbf{k}}. \tag{B3}$$

Let us now look at the interaction Hamiltonian,

$$H_I = U_0\int d^2r\,\hat{\phi}^4. \tag{B4}$$

After normal ordering, H_I contains the following generic terms:

$$(\hat{c}_{\mathbf{k}})^4, (\hat{c}^\dagger_{\mathbf{k}})^4, \hat{c}^\dagger_{\mathbf{l}}\hat{c}^\dagger_{\mathbf{p}}\hat{c}^\dagger_{\mathbf{q}}\hat{c}_k, \hat{c}^\dagger_{\mathbf{k}}\hat{c}_{\mathbf{l}}\hat{c}_{\mathbf{p}}\hat{c}_{\mathbf{q}}, \hat{c}^\dagger_{\mathbf{k}}\hat{c}^\dagger_{\mathbf{l}}\hat{c}_{\mathbf{p}}\hat{c}_{\mathbf{q}}. \tag{B5}$$

One can see that the first four terms of the list above are associated with field components [see Eq. (9)] that rotate as $e^{-4i(\mathbf{k}\cdot\mathbf{r}-\omega_{\mathbf{k}}t)}$, $e^{+4i(\mathbf{k}\cdot\mathbf{r}-\omega_{\mathbf{k}}t)}$, $e^{i(\mathbf{l}+\mathbf{p}+\mathbf{q}-\mathbf{k})\cdot\mathbf{r}-i(\omega_{\mathbf{l}}+\omega_{\mathbf{p}}+\omega_{\mathbf{q}}-\omega_{\mathbf{k}})t}$, and $e^{-i(\mathbf{l}+\mathbf{p}+\mathbf{q}-\mathbf{k})\cdot\mathbf{r}+i(\omega_{\mathbf{l}}+\omega_{\mathbf{p}}+\omega_{\mathbf{q}}-\omega_{\mathbf{k}})t}$, respectively. In these terms, due to conservation of energy and momentum, the exponents never vanish in scattering processes from a hard field potential. It is, thus, clear that the fifth term is, in general, the dominant one since the other terms will be spatially and temporally averaged out during the evolution of the condensate. We, therefore, retain only the last term $\hat{c}^{\dagger}_{\mathbf{k}}\hat{c}^{\dagger}_{\mathbf{l}}\hat{c}_{\mathbf{p}}\hat{c}_{\mathbf{q}}$ in the normal-ordered Hamiltonian [Eq. (B4)]. This procedure is standard and is conventionally used when treating nonrelativistic Hamiltonians [40]. Considering the fifth term only, we obtain the momentum conserving interaction Hamiltonian in momentum space,

$$H_I = \frac{U_0}{2A}\sum_{\mathbf{klp}} \frac{1}{\sqrt{\mathcal{E}_{\mathbf{k}}\mathcal{E}_{\mathbf{l}}\mathcal{E}_{\mathbf{l}+\mathbf{p}}\mathcal{E}_{\mathbf{k}-\mathbf{p}}}}\hat{c}^{\dagger}_{\mathbf{k}}\hat{c}^{\dagger}_{\mathbf{l}}\hat{c}_{\mathbf{l}+\mathbf{p}}\hat{c}_{\mathbf{k}-\mathbf{p}}. \tag{B6}$$

APPENDIX C: MULTIPLE SCALE PERTURBATION THEORY FOR THE NLKGE

In this Appendix, we introduce the multiple scale method for the nonlinear Klein-Gordon equation to show how the traveling waves propagates in a heterolayer condensate. For simplicity, we limit our analysis on one side of the condensate since the dynamics is the same on both sides,

$$\partial_\tau^2\psi - \left(\partial_\xi^2 + \partial_\eta^2\right)\psi + m^2\psi + \psi^3 = 0, \tag{C1}$$

with initial conditions,

$$\begin{aligned}\psi(\xi,\eta,0) &= \psi_0(\xi,\eta),\\ \psi_\tau(\xi,\eta,0) &= \psi_1(\xi,\eta),\end{aligned} \tag{C2}$$

we set a slow space-timescale $\xi_1 = \epsilon\xi$, $\eta_1 = \epsilon\eta$, and $\tau_1 = \epsilon\tau$. We can now make the following ansatz of a perturbation series for the solution:

$$\psi(\xi,\eta,0) = \sum_n \epsilon^{n+1}\Psi_n(\xi,\xi_1,\eta,\eta_1,\tau,\tau_1,\tau_2). \tag{C3}$$

Modifying the derivatives accordingly to the slow scale transformations and inserting the ansatz, the wave equation (C1), up to the second order, becomes (we will implicitly assume that initial conditions must be met at each order)

$$\epsilon\mathcal{L}_{\mathrm{KG}}(\Psi_0) + \epsilon^2[\mathcal{L}_{\mathrm{KG}}(\Psi_1) - 2\Psi_{0,\tau_1\tau} + 2\Psi_{0,\xi_1\xi}] + O(\epsilon^3) = 0, \tag{C4}$$

where $\mathcal{L}_{\mathrm{KG}} = \Box - m^2$ is the linear Klein-Gordon operator.

The order ϵ gives $\mathcal{L}_{\mathrm{KG}}(\Psi_0) = 0$, that is solved by a function of the form

$$\Psi_0(\xi,\xi_1,\eta,\eta_1,\tau,\tau_1) = A(\xi_1,\eta_1,\tau)e^{i(k_\xi\xi+k_\eta\eta-\omega\tau)} + \text{c.c.}, \tag{C5}$$

with the dispersion relation $\omega(k) = \sqrt{k^2+m^2}$, $k = (k_\xi, k_\eta)$. Proceeding to the following order we get:

$$\mathcal{L}_{\mathrm{KG}}(\Psi_1) = 2i(\omega A_\tau + k_\xi\partial_{\xi_1}A + k_\eta\partial_{\eta_1}A)e^{i(k_\xi\xi+k_\eta\eta-\omega\tau)} + \text{c.c.}, \tag{C6}$$

this term has the same structure as the solution to the homogeneous problem, and it, thus, represents a secularity and needs to be eliminated. This leads to the following condition on the amplitude $A(\xi_1,\eta_1,\tau)$:

$$\omega A_\tau + k_\xi\partial_{\xi_1}A + k_\eta\partial_{\eta_1}A = 0, \tag{C7}$$

and a solution of this equation is a unidirectional traveling wave of the form $A = A(\boldsymbol{\rho}_1 - v\tau_1)$ where $\boldsymbol{\rho}_1 = (\xi_1,\eta_1)$ and $\mathbf{v} = (v_\xi, v_\eta)$ is the group-velocity vector. This explains the behavior in Figs. 7 and 8 where we see unidirectional waves propagating along the ξ direction only since the initial momentum along η is set to zero.

[1] C. C. Bradley, C. A. Sackett, J. J. Tollett, and R. G. Hulet, Evidence of Bose-Einstein Condensation in an Atomic Gas with Attractive Interactions, Phys. Rev. Lett. **75**, 1687 (1995).

[2] M. H. Anderson, J. R. Ensher, M. R. Matthews, C. E. Wiemann, and E. A. Cornell, Observation of Bose-Einstein Condensation in a Dilute Atomic Vapor, Science **269**, 198 (1995).

[3] M. Grether, M. de Llano, and G. A. Baker, Jr., Bose-Einstein Condensation in the Relativistic Ideal Bose Gas, Phys. Rev. Lett. **99**, 200406 (2007).

[4] Lin J. L. and J. P. Wolfe, Bose-Einstein Condensation of Paraexcitons in Stressed CU_2O, Phys. Rev. Lett. **71**, 1222 (1993).

[5] J. M. Blatt, K. W. Böer, and W. Brandt, Bose-Einstein condensation of excitons, Phys. Rev. **126**, 1691 (1962).

[6] M. Combescot, R. Combescot, and F. Dubin, Bose-Einstein condensation and indirect excitons: A review, Rep. Prog. Phys. **80**, 0066501 (2017).

[7] I. B. Spielman, J. P. Eisenstein, L. N. Pfeiffer, and K. W. West, Resonantly Enhanced Tunneling in a Double Layer Quantum Hall Ferromagnet, Phys. Rev. Lett. **84**, 5808 (2000).

[8] L. V. Butov, A. C. Gossard, and D. S. Chemla, Towards Bose-Einstein condensation of excitons in potential traps, Nature (London) **417**, 47 (2002).

[9] L. V. Butov, C. W. Lai, A. L. Ivanov, and A. C. Gossard, and D. S. Chemla, Macroscopically ordered state in an exciton system, Nature (London) **418**, 751 (2002).

[10] D. Nandi, A. D. K. Fink, J. P. Eisenstein, L. N. Pfeiffer, and K. W. West, Exciton condensation and perfect Coulomb drag, Nature (London) **488**, 481 (2012).

[11] R. Balili, V. Hartwell, D. Snoke, L. N. Pfeiffer, and K. W. West, Bose-Einstein Condensation of microcavity polaritons in a Trap, Science **316**, 1007 (2007).

[12] X. Liu, K. Watanabe, T. Taniguchi, B. I. Halperin, and P. Kim, Quantum Hall drag of exciton condensate in graphene, Nat. Phys. **13**, 746 (2017).

[13] A. Kogar *et al.*, Signatures of exciton condensation in a transition metal dichalcogenides, Science **358**, 1314 (2017).

[14] T. Stroucken, J. H. Grönqvist, and S. W. Koch, Optical response and ground state of graphene, Phys. Rev. B **84**, 205445 (2011).

[15] A. S. Rodin and A. H. Castro Neto, Excitonic collapse in semiconducting transition-metal dichalcogenides, Phys. Rev. B **88**, 195437 (2013).

[16] T. Stroucken, and S. W. Koch, Optically bright p-excitons indicating strong Coulomb coupling in transition-metal dichalcogenides, J. Phys.: Condens. Matter **27**, 345003 (2015).

[17] S. Kembt *et al.*, Exciton-polariton topological insulator, Nature (London) **562**, 552 (2018).

[18] Z. Wang, N. Hao, Z. G. Fu, and P. Zhang, Excitonic condensation for the surface states of topological insulator bilayers, New J. Phys. **14**, 063010 (2012).

[19] J. I. A. Li, T. Taniguchi, K. Watanabe, J. Hone, and C. R. Dean, Excitonic superfluid phase in double bilayer graphene, Nat. Phys. **13**, 751 (2017).

[20] Z. Wang, M. W. Tu, Q. Tong, and W. Yao, Gate tuning from exciton superfluid to quantum anomalous Hall in van der Waals heterobilayer, Sci. Adv. **5**, 6120 (2019).

[21] S. Fagnocchi, S. Finazzi, S. Liberati, M. Kormos, and A. Trombettoni, Relativistic Bose-Einstein condensates: A new system for analog models of gravity, New J. Phys. **12**, 0950112 (2010).

[22] E. Farhi, N. Graham, V. Khemani, R. Markov, and R. Rosales, An oscillon in the SU_2 gauged Higgs model, Phys. Rev. D **72**, 101701(R) (2005).

[23] S.-W. Su, S.-C. Gou, I.-K. Liu, A. S. Bradley, O. Fialko, and J. Brand, Oscillons in coupled Bose-Einstein condensates, Phys. Rev. A **91**, 023631 (2015).

[24] N. N. Rosanov, N. A. Veretenov, N. V. Vysotina, L. A. Nesterov, S. V. Fedorov, and A.N. Shatsev, Oscillons of Bose-Einstein condensate, Opt. Spectrosc. **119**, 363 (2015).

[25] P. B. Umbanhowar, F. Melo, and H. L. Swinney, Localized excitations in a vertically vibrated granular layer, Nature (London) **382**, 793 (1996).

[26] H. Arbell, and J. Fineberg, Temporally Harmonic Oscillons in Newtonian Fluids, Phys. Rev. Lett. **85**, 756 (2000).

[27] O. Lioubashevski, Y. Hamiel, A. Agnon, Z. Reches, and J. Fineberg, Oscillons and Propagating Solitary Waves in a Vertically Vibrated Colloidal Suspension, Phys. Rev. Lett. **83**, 3190 (1999).

[28] I. V. Barashenkov, and E. V. Zemlyanaya, Soliton complexity in the damped-driven nonlinear Schrödinger equation: Stationary to periodic to quasiperiodic complexes, Phys. Rev. E **83**, 056610 (2011).

[29] I. V. Barashenkov, E. V. Zemlyanaya, and T. C. van Heerden, Time-periodic solitons in a damped-driven nonlinear Schrödinger equation, Phys. Rev. E **83**, 056609 (2011).

[30] A. O. Leon, M. G. Clerc, and D. Altbir, Dissipative magnetic breathers induced by time-modulated voltages, Phys. Rev. E **98**, 062213 (2018).

[31] A. J. Alvarez-Socorro, E. B. Berrios-Caro, M. G. Clerc, and A. O. Leon, Transition from nonradiative to radiative oscillons in parametrically driven systems, Phys. Rev. E **101**, 052209 (2020).

[32] M. Trushin, M. O. Goerbig, and W. Belzig, Optical absorption by Dirac excitons in single-layer transition-metal dichalcogenides, Phys. Rev. B **94**, 041301(R) (2016).

[33] D. N. Carvalho, A. Marini, and F. Biancalana, Dynamical centrosymmetry breaking - A novel mechanism for second harmonic generation in graphene, Ann. Phys. (NY) **378**, 24 (2017).

[34] D. N. Carvalho, F. Biancalana, and A. Marini, The nonlinear effects of opening a gap in graphene, Phys. Rev. B **97**, 195123 (2018).

[35] L. Meckbach, T. Stroucken, and S. W. Koch, Influence of the effective layer thickness on the ground-state and excitonic properties of transition-metal dichalcogenide systems, Phys. Rev. B **97**, 035425 (2018).

[36] L. Di Mauro Villari, I. Galbraith, and F. Biancalana, Coulomb effects in the absorbance spectra of two-dimensional Dirac materials, Phys. Rev. B **98**, 205402 (2018).

[37] D. S. Novikov, Elastic scattering theory and transport in graphene, Phys. Rev. B **76**, 245435 (2007).

[38] L. V. Keldysh, and A. N. Kozlov, Collective properties of excitons in semiconductors, Zh. Eksp. Teor. Fiz. **54**, 978 (1968).

[39] R. Wang, O. Erten, B. Wang, and D. Y. Xing, Prediction of a topological $p + ip$ excitonic insulator with parity anomaly, Nat. Commun. **10**, 210 (2019).

[40] S. A. Moskalenko, and D. W. Snoke, *Bose-Einstein Condensation of Excitons and Biexcitons* (Cambridge University Press, Cambridge, U.K., 2000).

[41] A. Aiello, Field theory of monochromatic optical beams: I. Classical fields, J. Opt. **22**, 014001 (2020).

[42] T. D. Lee, K. Huang, and C. N. Yang, Eigenvalues and eigenfunctions of a Bose system of hard spheres and its low-temperature properties, Phys. Rev. **106**, 1135 (1957).

[43] A. H. Castro Neto, F. Guinea, N. M. R. Peres, K. S. Novoselov, and A. K. Geim, The electronic properties of graphene, Rev. Mod. Phys. **81**, 109 (2009).

[44] M. Hindmarsh, and P. Salmi, Numerical investigations of oscillons in 2 dimensions, Phys. Rev. D **74**, 105005 (2006).

[45] E. J. Copeland, M. Gleiser, and H. R. Müller, Oscillons: Resonant configurations during bubble collapse, Phys. Rev. D **52**, 1920 (1995).

[46] E. P. Honda, and M. W. Choptuik, Fine structure of oscillons in the spherically symmetric φ^4 Klein-Gordon model, Phys. Rev. D **65**, 084037 (2002).

[47] T. Matos Honda, and A. Suárez, Finite temperature and dissipative corrections to the Gross-Pitaevskii equation from $\Lambda\Phi^4$, Europhys. Lett. **96**, 56005 (2011).

[48] S. Kasuya, M. Kawasaki, and F. Takahshi, I-balls, Phys. Lett. B **559**, 99 (2003).

[49] G. Moody, J. Schaibley, and X. Xu, Exciton dynamics in monolayer transition metal dichalcogenides, J. Opt. Soc. Am. B **33**, C39 (2016).

[50] D. J. Brown, A. V. H. McPhail, D. H. White, D. Baillie, S.K. Ruddell, and M. D. Hoogerland, Thermalization, condensate growth, and defect formation in an out-of-equilibrium Bose gas, Phys. Rev. A **98**, 013606 (2018).

[51] A. R. Fritsch, M. Lu, G. H. Reid, A. M. Pineiro, and I. B. Spielman, Creating solitons with controllable and near-zero velocity in Bose-Einstein condensates, Phys. Rev. A **101**, 053629 (2020).

[52] E. Y. Sherman, P. Lemmens, B. Busse, A. Oosawa, and H. Tanaka, Sound Attenuation Study on the Bose-Einstein Condensation of Magnons in $TlCuCl_3$, Phys. Rev. Lett. **91**, 057201 (2003).

[53] V. M. Pereira, V. N. Kotov, and A. H. Castro Neto, Supercritical Coulomb impurities in gapped graphene, Phys. Rev. B **78**, 085101 (2008).

[54] A. Das, *Lectures on Quantum Field Theory* (World Scientific, Singapore, 2008).